Environmental Research 222 (2023) 115310

Contents lists available at ScienceDirect

Environmental Research

journal homepage: www.elsevier.com/locate/envres

Thermodynamic characterization of LF, H, and mineral soil layers from oak forest ecosystems: Exploring the role of proximate analysis

Anika Seppelt [a,b], Juan Alberto Molina Valero [b], César Pérez-Cruzado [b], Nieves Barros [c,*]

[a] Faculty of Natural Sciences, Mathematics and Statistics, Ruprecht-Karls-Universität Heidelberg, 69117, Heidelberg, Germany
[b] PROEPLA, Higher Polytechnic School of Engineering, Campus Terra, 27002, Lugo, Spain
[c] Department of Applied Physics, Faculty of Physics, University of Santiago de Compostela, 15782, Santiago de Compostela, Spain

ARTICLE INFO

Keywords:
Soil
Thermal analysis
Proximate analysis
Energy

ABSTRACT

Studying the thermodynamic properties of soil organic matter is a developing field that involves the measurement of the energy stored by the soil. Quantifying soil energy content is still challenging despite different methodological approaches are available to calculate that value. One of the options is the proximate analysis following the guidelines for the energetic characterization of biomass. However, proximate analyses are still unexplored for soils. In this paper, we investigate the potential of this analysis to contribute to study soil from a thermodynamic perspective. With that goal, 31 soil samples collected in mature oak forests following a depth transect were used for elemental, thermal and proximate analysis. Proximate analyses and energetic characterization were performed by simultaneous thermogravimetry and differential scanning calorimetry.

These methods allowed fragmentation of the soil organic matter in water content, volatile matter, fixed carbon, and ash, as well as the quantification of the soil organic matter and energy content. Pearson's correlation showed significant relations among the proximate, the elemental components of soils and the energy. The equations relating all of these variables were calculated for soils from oak forests by partial least squares analysis. Equations representing the relationship between energy and the proximate fractions provide an additional alternative to calculate the heat of combustion of the soil organic matter. This value is the essential step for the thermodynamic characterization of soils.

1. Introduction

Soil, together with water, is one of the most important primary and essential resources for life on earth affected by multiple anthropological and environmental factors. Climate change and the increasing temperatures warm the soil causing heat flows and melting ice. Human pressure and the unsustainably high demands for resources to sustain human activity impact soil ecosystems. Given the necessity of energy, there is continuous research about sources and processes to yield new energy resources. Soil is not an exception, and the multiple soil management methods include it as a source of biomass for energy production involving the different ecosystems that soils sustain.

In search of energy resources, thermodynamic studies of the energy properties of a great sort of organic materials are performed by computing different models to yield their thermodynamic state functions, such as enthalpies, Gibbs energy, exergy, entropy and so on. The latter has been accounted for in specific organic substrates but not soils as such (Sarangi et al., 2018). The chemical characterization of soil organic matter (SOM) is facing methodological limitations because of its complex composition (Rumpel and Kögel-Knabner, 2011). The difficulties with characterizing SOM by specific chemical formulae have also prevented the chemical and stoichiometric study of most of the reactions taking place in and by soils until recently (LaRowe and Van Cappellen, 2011). Thermodynamics is one of the chemical tools for such a characterization. In this sense, soils are not yet characterized as a thermodynamic system, despite them being open systems interchanging energy and matter with the environment.

Until recently, monitoring of soil's processes has been developed only based on mass, but during the end of the 20th century and in particular the 21st century, the awareness of soil as a sink and a source of energy has begun, boosting scientific interest in that field (Barros et al., 2007; Chakrawal et al., 2021; Herrmann et al., 2014). This concept of soil as a sink and source of energy enables the consideration of soil in energy production (Smith et al., 2021) and knowledge development

* Corresponding author.
E-mail address: nieves.barros@usc.es (N. Barros).

https://doi.org/10.1016/j.envres.2023.115310
Received 8 September 2022; Received in revised form 14 December 2022; Accepted 13 January 2023
Available online 21 January 2023
0013-9351/© 2023 The Authors. Published by Elsevier Inc. This is an open access article under the CC BY-NC-ND license (http://creativecommons.org/licenses/by-nc-nd/4.0/).

about how soil manages energy to sustain the carbon cycle (Chakrawal et al., 2021) and how it is involved in the evolution of soil ecosystems. Thermodynamics has usually played a traditional theoretical role in these fields (Hansen et al., 2018; Odum, 1969).

Technological advances make the thermodynamic characterization of soils a realistic goal. There is, however, practically no previous knowledge about the quantification of the thermodynamic variables for soil systems and reactions, being essential the search for the best methods and developments. The most basic goal towards the soil thermodynamic characterization is the quantification of the energy content of SOM, which is still challenging. Typically, bomb calorimetry is used to quantify the energy stored in organic substrates by parameters such as heat of combustion (Q) or enthalpy of combustion (H) (Villanueva et al., 2010). However, this method fails when applied to mineral soils (Rovira and Henriques, 2011). Additional methods are arising from the application of different enthalpic models and thermogravimetry. A recent study compared their application to soil samples (Malucelli et al., 2020). One of them is the application of proximate analysis and the calculation of models explaining the energy content of SOM by its composition (Huang et al., 2022).

Proximate analysis is applied to biomass and biochar (Klasson, 2017). It fractionates the organic matter in volatile matter (VM), fixed carbon (FC) and ash (A), but there are no data for soils yet. SOM has been traditionally fractionated in labile, recalcitrant and refractory thermal fractions by thermogravimetry (Dell'Abate et al., 2000; Fernández et al., 2012). However, this thermal fractionation did not enable quantifying SOM energy, whereas this is possible with proximate analysis, which is one of the existing approaches for thermodynamic characterization of biomass nowadays, using models that describe energy and exergy of organic substrates with the data of proximate analysis (Huang et al., 2022).

It would be interesting to study the reliability of proximate analysis for characterizing SOM to include it as a tool to study SOM evolution and as an alternative to calculate SOM energy content as applied to other organic resources.

This paper explores the validity of those methods for characterizing SOM by combining elemental SOM composition with simultaneous thermogravimetry and differential scanning calorimetry. It also studies the sensitivity of the proximate fractions to SOM evolution from the soil surface to the mineral soil with samples from different geographical locations.

2. Materials and methods

2.1. Soil samples

Soil samples come from different geographical locations in Ireland, the UK, France, and Portugal. All of them were collected in mature oak forest ecosystems.

Samples from Ireland and UK have been defined in previous papers (Barros, 2021; Barros et al., 2020). They were collected at three different locations in Ireland and UK. Samples from France were collected at five different locations. The sample from Portugal represents only one sampling site. Table S1 summarizes the sampling locations, the soil types and the different soil layers sampled at each location.

Sampling criteria were common for all sampling sites and are explained in detail in previous work (Barros et al., 2020). The soil was collected at different depths. A square of 0.25 × 0.25 m was used to collect the loose litter (L) and fermented (F) layer (samples LF). The humic layer (H samples) was collected with a hammering head and stainless steel rings of 100 cm^3 of volume. This H layer was not presented in all sampling sites. However, it was possible to collect it for all sites from Ireland, four in France and one in Portugal. After removing the entire H layer, the same process was used to collect mineral soil samples at the top 5 cm of the mineral layer (M samples).

All soil samples were air-dried at laboratory temperature. LF and H samples were ground, and the mineral samples were sieved through 2 mm.

2.2. Soil elemental analysis

Elemental analysis of Carbon (C), Hydrogen (H) and Nitrogen (N) was done with a CHNS LECO analyser (TrusPec CHNS). Organic carbon (C_{org}) was measured with a THERMO FLASHSMART analyser (Thermoscientific flashsmart) after removing inorganic carbon with HCl 1:1.

The oxygen content (O) was measured by performing Nickel-tube pyrolysis in a reactor at 1060 °C. Oxygen combined with carbon yields CO which is measured by chromatography (Saurer and Siegwolf, 2004). Data were analysed by the Eager Xperience software.

2.3. Thermal analysis

Soil thermal properties were studied by simultaneous thermogravimetry and differential scanning calorimetry (TG-DSC) with a TGA-DSC1 (Mettler-Toledo). The soil organic matter content (SOM) and the heat of combustion of SOM (Q_{SOM}) were determined by TG-DSC under a temperature scan ranging from 50 °C to 600 °C with 10 °C per minute under dry airflow at 50 ml per minute after previous calibration of the device.

SOM pyrolysis was performed by TG-DSC under a temperature scan from 50 °C to 600 °C with 10 °C per minute and Nitrogen flow (N-flow) at 50 ml per minute. The soil mass remaining after pyrolysis was analysed by a subsequent scan at the same temperatures and rates under dry airflow again at 50 ml per minute.

2.4. Calculations

The initial weights (m_0) of the soil samples were measured before the combustions. The dry weight (m_{dw}) of the samples is considered as the weight at 180 °C and thus after evaporation of the water. For comparability, the following values are given as percentages of the sample dry mass (m_{dw}).

The water content or moisture (M) as percentage of the initial mass (m_0) is defined as the mass loss (ML) between 50 °C and 180 °C:

$$M = (m_0 - m_{180°C}) * 100 / m_0 \quad (1)$$

The residual mass that remains after the combustion under airflow (weight at 600 °C: $m_{600°C}$) normalized to the m_{dw} is considered as the percentage of mineral char (A_{air}):

$$A_{air} = m_{600°C} * 100/m_{dw} \quad (2)$$

As comparison, the residual mass after the pyrolysis and subsequent combustion was measured similarly and is called A_{N+air} hereinafter. The SOM content was determined in the combustion under airflow and was calculated as the difference between A_{air} ($m_{600°C}$) and dry weight (m_{dw}):

$$m_{SOM} = m_{dw} - m_{600°C} \quad (3)$$

Thus, SOM is calculated as a percentage too:

$$SOM(\%) = m_{SOM} * 100/m_{dw} \quad (4)$$

Furthermore, the combined combustions under the flow of nitrogen (pyrolysis) and subsequently flow of dry air, yield the percentages of volatile SOM (VM) and fixed carbon (FC) which compose the SOM. VM is the mass pyrolyzed from 180 °C to 600 °C and is directly determined in the TG trace obtained under the N_2 atmosphere:

$$VM = (m_{N180°C} - m_{N600°C}) * 100 / m_{N180°C} \quad (5)$$

The fixed carbon (FC) is defined as the carbon remaining after the pyrolysis. It can be calculated by (Malucelli et al., 2020):

$$FC_{calc} = 100 - M - VM - A_{air} \quad (6)$$

where A_{air} is the mineral char after combustion under airflow. We propose to simplify the calculation to:

$$FC_{calc} = SOM - VM \quad (7)$$

According to its definition as the carbon remaining after pyrolysis, the FC can also be experimentally determined. Hence, it is the ML during the combustion under airflow after the pyrolysis. Therefore FC_{exp} is considered as the difference between the residual mass of the pyrolysis ($m_{N600°C}$) and the residual mass of the second combustion ($m_{N+air600°C}$) normalized to the dry weight before the pyrolysis ($m_{N180°C}$) (Chouchene et al., 2010):

$$FC_{exp} = (m_{N600°C} - m_{N+air600°C}) * 100 \,/\, m_{N180°C} \quad (8)$$

Combustion by simultaneous TG-DSC measures the energy of the SOM, which is released concomitantly to the mass combustion and pyrolysis. The reaction under airflow allows to determine the heat of combustion relative to the mass of SOM of each sample (Q_{SOM} in kJ/g of SOM), also called Higher Heating Value (HHV) (Huang et al., 2022) after Baraldi's correction (Barros et al., 2020). Q_{SOM} is directly obtained by integrating the DSC plots in Watts normalized to SOM content (m_{SOM}) versus time in seconds after baseline correction (Barros et al., 2020; Fernández et al., 2012).

2.5. Statistical analysis

Comparison of data from the different soil layers was done by a paired sample *t*-test when the data followed a normal distribution and homoscedasticity. Data that did not fulfil the normality test were compared by the Kruskal-Wallis ANOVA test. Comparison of the same data obtained by different procedures that did not fulfil the normality test was done by the paired sample Wilcoxon signed-rank Test (PSWRT). Relation among variables was studied by Pearson's correlations. Multiregression analysis was done by the paired least square method. Clustering of samples based on different variables was performed by K-means cluster analysis. The analyses were done by OriginPro software (OriginPro, 2022) and by RStudio software.

3. Results

3.1. Soil thermal and elemental properties

3.1.1. Elemental composition of soil samples

Soil elemental components C, H and N, together with the organic carbon (C_{org}) and Oxygen (O), are shown in Table 1. There is a clear trend of all these components to decrease with increasing soil depth, i.e., from the horizons LF to the M.

3.1.2. Thermal characterization of soil samples

Derivative thermogravimetry (DTG) plots show that all samples follow a similar profile after combustion and pyrolysis (Fig. 1). DTG under airflow yields plots with two peaks in most LF samples. The first peak is found at temperatures ranging from 298 to 319 °C for all LF samples. The second peak occurs from 397 to 429 °C. A few samples have a third peak at 462 to 483 °C (i.e., EBW, F1 and F5), corresponding to the temperature of ash formation. The evolution of SOM from LF to H and M samples did not alter this profile. However, H and M samples do not show the third peak, and the two peaks of M samples occur at generally lower temperatures than those of LF and H samples (see Table 2). These peak temperatures represent the temperatures at which the rate of mass loss per time (dm/dt) reaches a maximum. Therefore, the peaks of the DTG under airflow indicate combustion processes of fractions of SOM with different thermal stability, allowing the fragmentation of SOM in different thermal Exo fractions (see Fig. 2).

The Exo 1 fraction represents the soil mass combusted at temperatures lower than 380 °C commonly attached to labile material like carbohydrates and proteins. The Exo2 fractions is the soil mass combusting

Table 1
Soil elemental and energetic properties. Values of total carbon (C_{tot}), organic carbon (C_{org}), Nitrogen (N), Hydrogen (H) and Oxygen (O) as percentages of the mass of the soil samples, together with the heat of combustion of SOM determined under air flow (Q_{SOM}) and the heat of combustion of the pyrolyzed soil (Q_{SOM} N + Air) are shown.

Samples	Horizon	C_{tot} (%)	C_{org} (%)	N (%)	H (%)	O (%)	Q_{SOM} (kJ/gSOM)	Q_{SOM} (N + Air) (kJ/gSOM)
EBW	LF	44,11	40,72	2,36	5,52	32,08	−16,48	−36,06
ERG	LF	42,58	34,21	1,83	4,44	31,94	−15,19	−28,20
ENF	LF	38,29	37,1	2,02	4,59	31,02	−15,23	−31,00
IDC	LF	46,66	41,62	1,4	5,69	35,55	−15,17	−37,53
IG	LF	47,02	46,14	1,64	5,73	35,49	−16,15	−43,78
IK	LF	46,41	39,98	1,56	5,83	34,44	−15,51	−41,51
F1	LF	36,24	35,23	1,46	4,52	24,12	−17,37	−42,26
F2	LF	45,05	41,4	1,07	5,73	29,80	−15,51	−41,66
F3	LF	38,82	38,49	1,62	4,89	28,25	−16,49	−38,30
F4	LF	34,74	31,59	2,29	4,62	23,04	−17,41	−38,98
F5	LF	27,85	19,74	1,35	3,91	16,83	−18,35	−45,04
IDC	H	20,93	17,07	0,78	2,39	12,87	−15,50	−31,81
IG	H	12,53	11,73	0,5	2,3	12,87	−15,18	−27,80
IK	H	10,14	10,03	0,64	1,09	26,00	−15,34	−29,82
P	H	30,2	18,89	1,84	3,82	12,82	−18,08	−32,65
F2	H	29,14	27,75	1,32	3,83	18,28	−16,41	−36,37
F3	H	12,46	11,43	0,73	1,64	11,35	−17,21	−33,21
F4	H	28,68	25,68	1,91	3,91	20,41	−17,48	−36,34
F5	H	12,87	11,39	0,75	1,61	8,31	−18,22	−39,10
EBW	M	7,06	5,44	0,44	0,99	4,23	−17,1	−29,04
ERG	M	3,58	3,38	0,21	0,38	2,45	−18,83	−29,78
ENF	M	9,34	8,84	0,42	1,2	6,16	−17,69	−31,64
IDC	M	5,67	4,45	0,18	0,77	2,49	−19,69	−34,64
IG	M	4,82	4,72	0,24	0,69	2,50	−17,39	−36,51
IK	M	10,62	8,81	0,44	1,5	5,32	−19,60	−30,20
P	M	13,12	10,06	0,9	1,76	9,57	−18,1	−30,86
F1	M	1,71	1,61	0,16	0,38	2,50	−19,38	−52,00
F2	M	0,92	0,8	0,06	0,13	0,18	−23,22	−52,88
F3	M	1,54	1,44	0,11	0,22	0,90	−21,79	−44,14
F4	M	4,13	3,62	0,28	0,73	3,48	−17,81	−49,76
F5	M	2,43	2,37	0,15	0,37	3,24	−19,28	−44,79

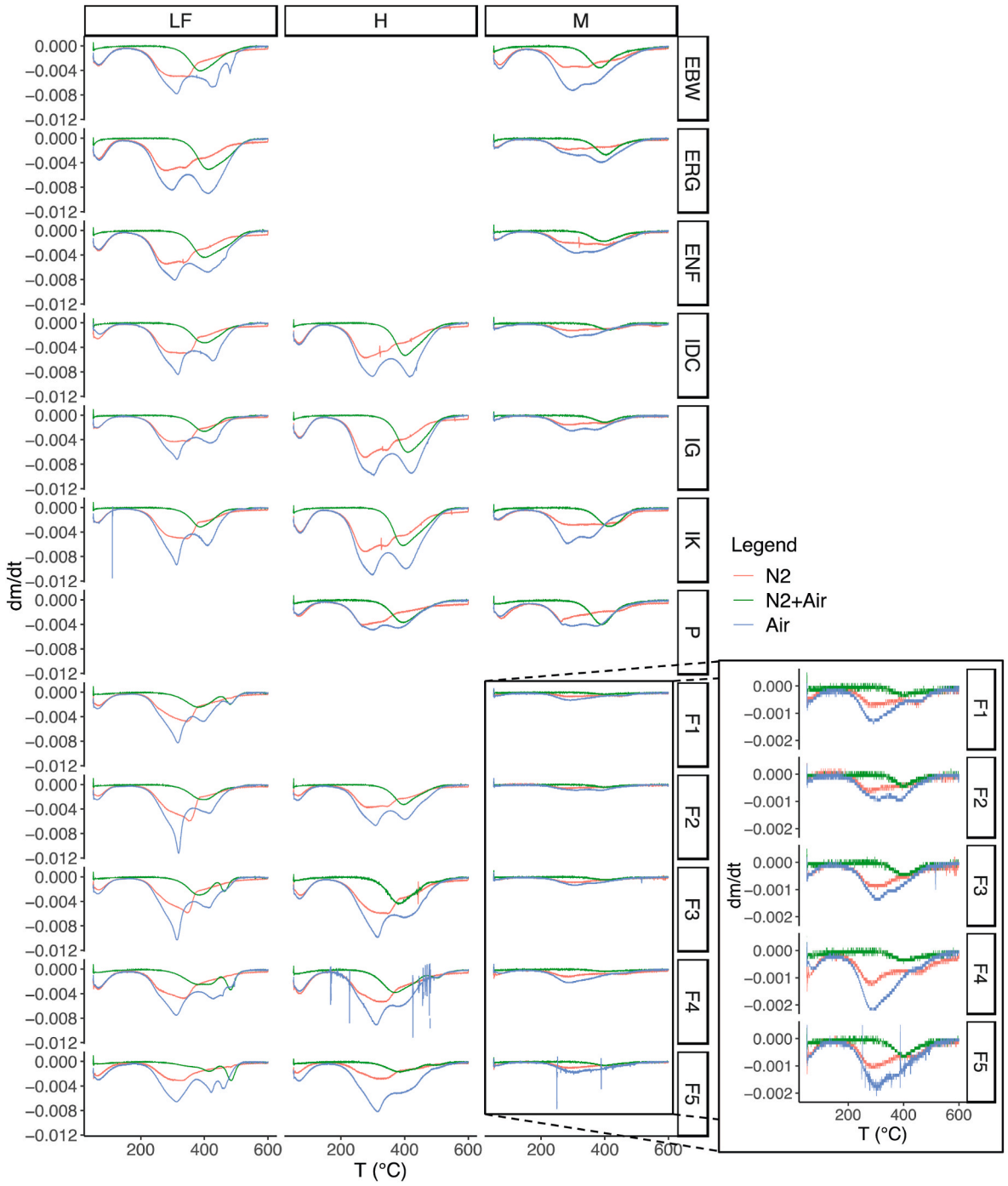

Fig. 1. DTG plots of the combustion under air flow (blue, Air), the pyrolysis (red, N_2) and the combustion after pyrolysis (green, N_2+Air) of all soil samples.

at temperatures ranging from 380 to 475 °C, attached to recalcitrant material like lignin and aromatic compounds. The Exo 3 fraction is the soil mass combusting at temperatures from 475 to 600 °C related to refractory material like black carbon (Dell'Abate et al., 2003, 2000). Most of the LF samples (Fig. 2) have higher Exo 1 than Exo2 fractions, with just two exceptions (ERG-LF and ENF-LF). Except for the sample P–H, the H samples show the same relative prevalence as their respective LF samples of Exo1 over Exo2. Samples from Ireland (IDC-H, IG-H, IK-H) show a clear depletion of the Exo 1 fraction compared with the values of their respective LF samples (Fig. 2). Mineral samples showed lower Exo 1 values than Exo 2 except for some of the samples from France (F samples), where Exo1 continues to be higher than the Exo2 fraction (F1-M, F3-M, F4-M and F5-M). There was no correlation between the Exo fractions and the soil elements. Therefore, it was not possible to attach the soil elemental composition to the different Exo fractions.

DTGs under N-flow (Fig. 1) showed different evolution of SOM pyrolysis. All LF samples show one main peak at temperatures that were similar to, or higher than, those obtained by combustion under airflow, varying from 279 to 351 °C (Table 2). In H samples, the pyrolysis DTG profile is more complex and varies with the sampling location. Samples from Ireland (IDC-H, IG-H, IK-H) show three different peaks at different temperatures, while samples from Portugal (P–H) and France (F2–H, F3–H, F4–H and F5–H) show a profile like those of their LF samples (except for the P sample). Mineral samples show one or two peaks in the DTG plots under N_2 (Table 2).

Table 2
Temperatures at the maxima of the DTG peaks (Fig. 1) obtained under airflow, under N-flow (Pyrolysis), and under airflow after pyrolysis for all the soil samples.

Samples	Horizon	Airflow [°C]			Pyrolysis (N-flow) [°C]			Airflow after Pyrolysis [°C]	
		T_1	T_2	T_3	T_1	T_2	T_3	T_1	T_2
EBW	LF	314	428	482	346			386	
ERG	LF	298	410		279	338	384	414	
ENF	LF	308	413		282	334		397	
IDC	LF	317	424		323	392		402	
IG	LF	312	416		307	344		398	
IK	LF	312	410		346	395		386	
F1	LF	317	397	483	345			379	480
F2	LF	319	416		351			406	
F3	LF	314	413		344			386	463
F4	LF	312	429		331			393	482
F5	LF	312	421	462	323			414	485
IDC	H	299	416		275	388		400	
IG	H	304	422		277	338	385	411	
IK	H	297	404		278	337	388	393	
P	H	298	379		269			397	
F2	H	308	400		287	345	395	397	
F3	H	314	395		346			381	
F4	H	308	371		327			372	502
F5	H	313	375		323			386	496
EBW	M	295	344		277	337		384	
ERG	M	314	383		279	340	389	404	
ENF	M	304	356		345	403		395	
IDC	M	289	342		300	560		412	
IG	M	289	366		282	396		400	
IK	M	278	344		309	393		417	
P	M	289	363		262	424		390	
F1	M	291	444		288	450		406	
F2	M	307	383		279	396		400	
F3	M	298	360		302			404	
F4	M	277			282	446		400	
F5	M	302	356		288	422		402	

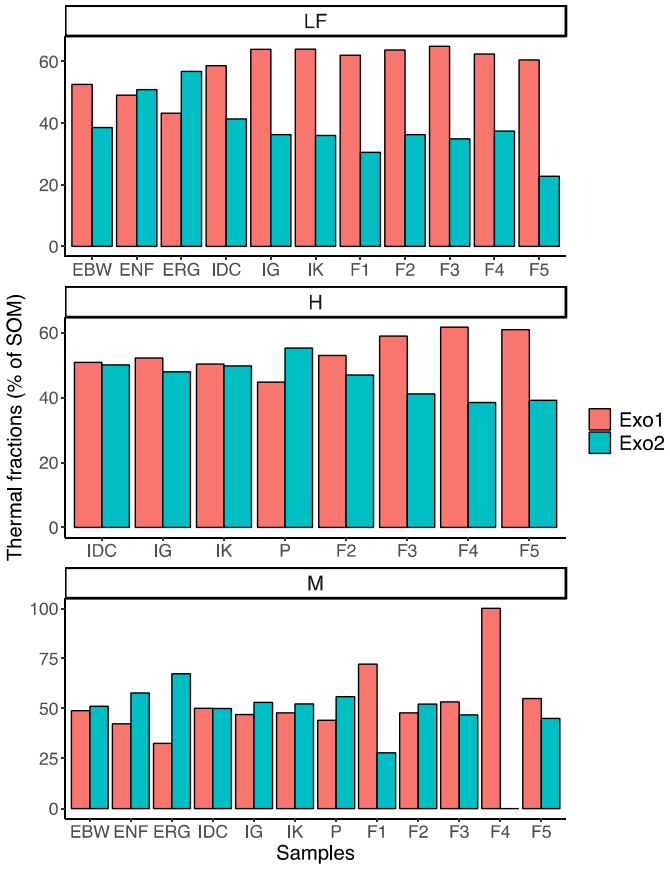

Fig. 2. Thermal fractions Exo 1 and Exo 2 of the soil samples are shown as percentage of the mass of SOM.

Combustion under airflow after the pyrolysis showed that all samples still have C in the material remaining after the pyrolysis. The combustion of that material yielded a single peak in all cases at temperatures ranging from 371 to 417 °C, except for the LF samples from France (F1, F3, F4 and F5) showing a second peak at similar temperatures to the observed third peak in the first combustion, corresponding to the temperature of ash formation (Table 2).

3.1.3. Heat of combustion

TG-DSC under airflow yields the heat of combustion (Q_{SOM}) of the samples (Table 1). A comparison of Q_{SOM} data between the LF and M samples showed that this value tends to increase as SOM evolves from LF to M soil layers. A paired sample *t*-test (two levels: LF and M samples, $n = 24$, $p < 0.05$) yielded a significant difference between the LF and M layers, indicating the trend of SOM to a more reduced state as soil depth increased (Fig. 3).

DSC of the matter remaining after pyrolysis yielded higher Q_{SOM} values than the original SOM (Table 1). Therefore, pyrolysis of SOM under the given conditions yields a higher energetic and more reduced material than the original SOM. This transformation did not show any correlation or trend corresponding to soil layers or geographical locations of samples.

3.2. Proximate analysis

TG under N_2 allows the calculation of soil water content (moisture M), and SOM fractionation in volatile organic matter (VM) and fixed carbon (FC), as well as ash quantification (A_{N+air}). Results are shown in Table 3.

Calculation of the fixed carbon (FC) by the reported formula ($FC = 100 - (M + VM + A)$) (Malucelli et al., 2020) simplified here as $FC_{calc} = SOM - VM$, where SOM is determined by the first airflow, gives data not significantly different from those given by the experimental procedure (FC_{exp}) (Chouchene et al., 2010), when compared by the Wilcoxon,

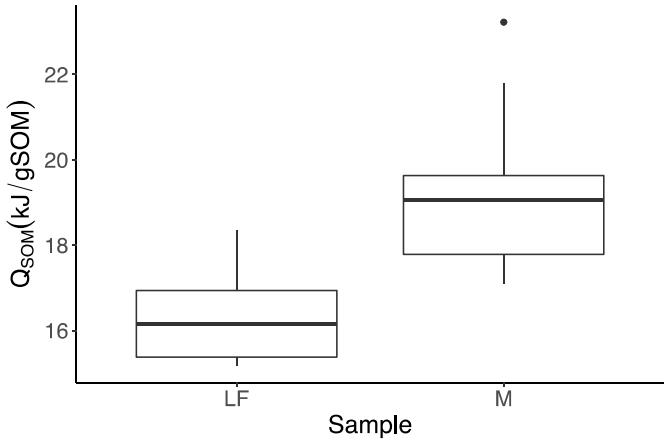

Fig. 3. Heat of combustion (Q_{SOM}) of LF and M samples. The absolute values of combustion Q_{SOM} are shown for better comparison (original values are shown in Table 1). M samples exhibit significantly higher heat of combustion values than LF samples ($p < 0.05$, obtained by a paired sample t-test). Points show observations out of ± 1.5 times the interquartile range.

Signed Ranks Test (WSRT) ($n = 62$, $p < 0.05$).

The percentage of ash after the first combustion (A_{air}) is not significantly different than the ash value obtained from the second combustion after the pyrolysis (A_{N+air}) when comparing with WSRT ($n = 62$, $p < 0.05$).

The volatile matter and the fixed carbon were normalized to the SOM content to study the contribution of both within SOM in the samples (VM_{SOM}; FC_{SOM}, Table 3). Fig. 4 shows the volatile matter (Fig. 4a) and the fixed carbon content (Fig. 4b) in the different soil horizons as a percentage of the SOM. The percentage of volatile matter increases from the horizons LF to M and, thus, with increasing depth. Consequently, the percentage of the fixed carbon decreases. There are significant differences between the volatile matter and the fixed carbon contents of the LF and the M horizon ($p < 0.05$, Kruskal-Wallis ANOVA test). These values for horizon H do not significantly differ from the respective content in the other two horizons. Besides being intermediate, the volatile matter and fixed carbon values of the horizon H have a great variance (Fig. 4).

3.3. Statistical comparison of the soil samples

3.3.1. K-means cluster analysis

K Clustering is constructed based on the thermal properties under airflow (Exo1, Exo2, Ash, SOM, and Q_{SOM}). Results show three groups, where group 2 is entirely constituted by the M samples with just one exception (EBW-M) and group 3 is entirely constituted by the LF samples. Half of the H samples are part of group 1 and the rest overlapped with group 2 (M samples) (Fig. 5a). When applied to proximate data, VM, FC and VM/FC ratio, distribution of samples in the plot (Fig. 5b) yielded three different groups too. No group was formed according to the geographical locations where samples were collected. Therefore, thermal properties just depended on the SOM evolution with depth.

3.3.2. Multiple regression analysis

Both, the volatile matter and the fixed carbon determined experimentally by N_2 and the subsequent air atmosphere were closely and significantly correlated to SOM determined by combustion under air ($n = 31$, $r = 0.98$, $r = 0.96$ respectively, $p < 0.001$) (Table S2). Therefore, the volatile matter and the fixed carbon are a function of the SOM percentage. The relation of the volatile matter to the fixed carbon is variable among samples. K-means cluster analysis based on the

Table 3
Results from proximate analysis: The soil organic matter, SOM, ash, A, volatile matter, VM, and fixed carbon, FC, contents of the soil samples are shown as percentage of the soils dry weight (m_{dw}). The formulas for the calculation of the SOM, ash content after the first combustion, A_{air}, volatile matter, VM, the theoretical fixed carbon, FC_{calc}, the experimental fixed carbon, FC_{exp}, (i.e. equations ((2), (4), (5), (7) and (8) respectively, and the ash content after the pyrolysis, A_{N+air}, are explained in section 2.3. VM_{SOM}, and FC_{SOM}, show the percentages of the volatile matter ~~VM~~ and the experimental fixed carbon, FC_{calc} respectively, normalized to the SOM content (see also Fig. 4).

Samples	Horizon	SOM	A_{air}	A_{N+air}	VM	FC_{calc}	FC_{exp}	VM_{SOM}	FC_{SOM}
EBW	LF	83,43	16,57	12,72	53,40	30,03	33,89	64,01	35,99
ERG	LF	71,87	28,13	34,26	39,73	32,13	26,01	55,29	44,71
ENF	LF	76,18	23,82	21,02	49,59	26,59	29,39	65,09	34,91
IDC	LF	93,36	6,64	6,29	60,20	33,16	33,52	64,48	35,52
IG	LF	92,93	7,07	4,64	63,47	29,45	31,89	68,30	31,70
IK	LF	93,60	6,40	5,72	62,27	31,33	32,01	66,53	33,47
F1	LF	75,93	24,07	22,03	48,34	27,59	29,63	63,66	36,34
F2	LF	92,17	7,83	9,23	60,18	31,99	30,60	65,29	34,71
F3	LF	84,77	15,23	16,81	54,50	30,27	28,68	64,29	35,71
F4	LF	75,79	24,21	23,36	45,79	29,99	30,85	60,42	39,58
F5	LF	65,55	34,45	50,77	29,48	36,07	19,75	44,98	55,02
IDC	H	93,40	6,60	12,79	54,88	38,52	32,33	58,76	41,24
IG	H	79,65	20,35	22,56	49,04	30,60	28,39	61,58	38,42
IK	H	87,05	12,95	14,29	54,66	32,39	31,06	62,79	37,21
P	H	36,45	63,55	51,90	29,09	7,36	19,01	79,81	20,19
F2	H	64,68	35,32	40,31	37,25	27,43	22,44	57,59	42,41
F3	H	35,34	64,66	63,69	23,47	11,87	12,84	66,41	33,59
F4	H	51,10	48,90	42,72	34,92	16,18	22,36	68,33	31,67
F5	H	30,77	69,23	81,26	11,49	19,28	7,26	37,33	62,67
EBW	M	24,45	75,55	77,44	14,18	10,27	8,38	57,98	42,02
ERG	M	9,39	90,61	89,97	5,54	3,85	4,49	58,98	41,02
ENF	M	17,32	82,68	81,07	12,57	4,74	6,36	72,60	27,40
IDC	M	5,94	94,06	93,43	4,40	1,55	2,17	73,98	26,02
IG	M	9,82	90,18	89,60	7,13	2,70	3,28	72,52	27,48
IK	M	19,89	80,11	77,25	15,16	4,74	7,59	76,18	23,82
P	M	18,52	81,48	75,61	14,29	4,23	10,10	77,18	22,82
F1	M	4,81	95,19	94,29	3,43	1,37	2,27	71,46	28,54
F2	M	2,14	97,86	97,58	1,39	0,75	1,03	64,73	35,27
F3	M	2,59	97,41	96,83	2,06	0,53	1,11	79,43	20,57
F4	M	7,76	92,24	91,97	5,70	2,06	2,33	73,44	26,56
F5	M	4,09	95,91	95,58	2,69	1,41	1,73	65,66	34,34

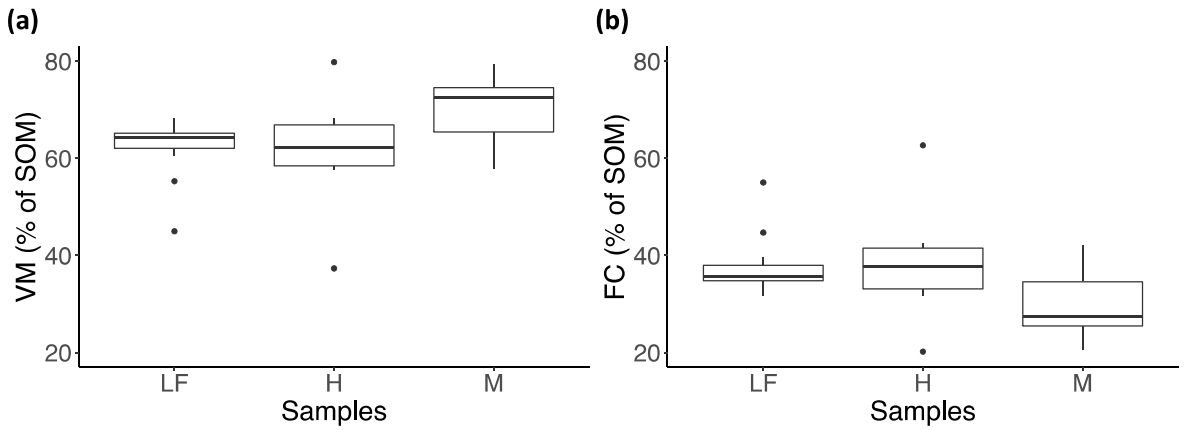

Fig. 4. Percentages of volatile matter, VM, and fixed carbon, FC, normalized to SOM content for LF, H and M samples. The percentage of volatile matter related to SOM is increasing from LF to M samples (figure a) while the fixed carbon is decreasing (figure b). The difference in the percentages of the volatile matter and the fixed carbon between LF and M samples is statistically significant ($p < 0.05$, Kruskal-Wallis test). Points show observations out of ±1.5 times the interquartile range.

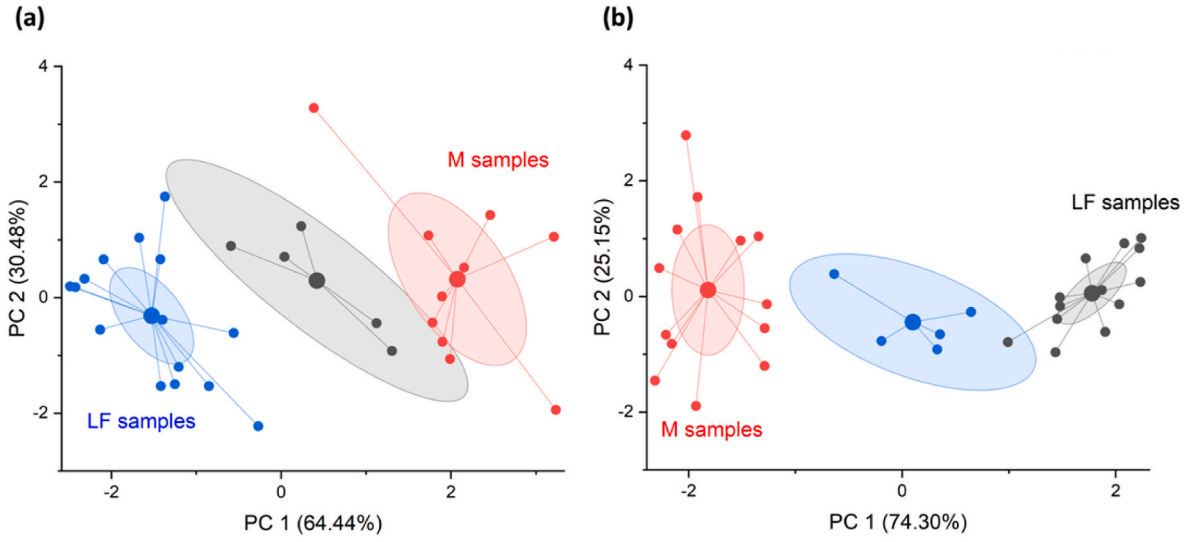

Fig. 5. K-means cluster plot data based on Exo1, Exo2, Ash, SOM and Q_{SOM} (a) and based on the volatile matter, VM, fixed carbon, FC, VM/FC ratio and SOM from all soil samples (b). The selected variables give two principal components (PC). PC1 explains 64.44% of the variance and PC2 30.48% for soil thermal properties under airflow (a). PC1 explains 74.30% of the variance and PC2 25.15% for the proximate data (b). Distribution of samples in the plots yields three different groups (indicated by colours red, blue and black).

proximate data (VM, FC, SOM, and VM/FC ratio) differentiated the LF samples from the M ones, with H samples overlapping with LF and M (Fig. 4).

Multi-regression analyses are applied to correlate the elemental, proximate and energetic properties of these soils, following the common procedures used for the energetic characterization of biomass. As a result, elemental properties were closely and significantly correlated to the proximate fractions, SOM and the energy content of samples (Table S2), validating the application of the partial least square method (PLS, see Table 4).

Soils have a highly organic component on the surface, but as it mineralizes, the mineral part starts to have an important effect on the ash content that alters the correlations. Pure organic substances yield low ash percentages, as happened here with the LF layers, but mineralization increases the prevalence of the ash fraction, which must be considered in the PLS analysis design. The energy content used for the PLSA is obtained by the integration of the DSC plots under airflow normalized to the dry weight of the sample combusted and named here as the Higher Heating Value (HHV), while Q_{SOM} is the value of the integral of the DSC plot normalized to the SOM content given by the TG under airflow. HHV data were used as the dependent variable for the PLS analysis, with the volatile matter, fixed carbon, and ash values as independent variables (see Table 4).

Table 4
Multiple linear regressions. Results of partial least square method for correlations among the soil elemental components and energy with the soil proximate fractions.

$C_{tot} = 0.694FC + 0.260VM + 1.252$	References (Parikh et al., 2007)
$C_{tot} = 0.887FC + 0.418VM + 0.888\ A – 15.726$	
$C_{org} = 0.201FC + 0.492VM + 0.544$	$C = 0.637FC + 0.455\ VM$
$C_{org} = 0.403FC + 0.657VM + 0.177\ A – 17.170$	$H = 0.052FC + 0.062\ VM$
$H = 0.084FC + 0.032VM + 0.266$	$O = 0.304\ FC + 0.476\ VM$
$H = 0.109FC + 0.053VM + 0.022\ A – 1.944$	
$O = 0.211FC + 0.391VM + 0.028$	
$O = 0.284FC + 0.450VM + 0.065\ A – 6.426$	
$HHV = -0.641\ FC + 0.961\ VM – 2.439$	
$HHV = -0.987\ FC + 0.680\ VM – 0.304\ A + 27.934$	

In the case of soils, hydrogen, H, and oxygen, O, were the elements giving equations closer to the references (Parikh et al., 2007) when considering the effect of the ash fraction (reference equations in

Table 4). C is the element with more variable results. Correlations with proximate fractions are positive in all cases, indicating that all variables depend on the SOM mass. Correlations with HHV are very variable in the literature. In this case, samples with lower energy content (HHV) present more oxidizable carbon (FC) and ash, while higher energy involves more VM. HHV obtained from proximate fractions should be normalized to the SOM percentage to yield the Q_{SOM} of the samples.

4. Discussion

DSC-TG under airflow is traditionally applied to characterize the thermal properties of SOM (Dell'Abate et al., 2003, 2000; Lopez-Capel et al., 2005; Plante et al., 2009). This method fractionates SOM based on the temperatures of the different combustion peaks given by the DTG and DSC plots. The profiles obtained with samples in this paper show that SOM components typically combust at the peak temperatures reported for labile SOM (celluloses and hemicellulose, temperatures ranging from 200 to 380 °C), recalcitrant substrates (lignin and their aromatic derivates, temperatures ranging from 380 to 475 °C), and also refractory SOM (temperatures from 475 to 600 °C) in some of the samples (De la Rosa et al., 2008). These peak temperatures allow the quantification of the percentages of labile, recalcitrant and refractory SOM contributing to the total SOM macromolecule, defined here as Exo1, Exo2 and Exo 3 fractions respectively (Dell'Abate et al., 2003, 2000). The DTG and DSC plots of the samples in this paper show different profiles as soil depth increases, indicating changes in the thermal properties usually corresponding to a differing chemical nature (Lopez-Capel et al., 2005; Manning et al., 2005). All LF samples with SOM at a low degree of decomposition show similar DSC and DTG plots, with bimodal curves and well-differentiated temperature peaks indicating labile and recalcitrant SOM such as lignocellulosic material. These samples show a clear relative prevalence of Exo1 over Exo2 fractions. H samples keep a similar profile in the DSC and DTG plots to the respective LF profiles, but the analysis of the percentage of the Exo fractions indicates how SOM evolved. Since the percentage of Exo1 fractions of all H samples is lower than the respective Exo1 fraction of LF samples, it can be suggested that the decomposition of the labile material (cellulose, hemicellulose, proteins, carbohydrates) is faster than that of recalcitrant material (mainly lignin) (Almendros and González-Vila, 2012; Merino et al., 2014). M samples show higher variability of these SOM properties. Most of the mineral soils have higher Exo2 than Exo1 content, while in a few samples, the Exo1 fraction still prevails. Other samples have just one fraction corresponding to labile material. The evolution of these data indicates how SOM evolved with increasing depth towards a more transformed SOM with different chemical properties. The results also show geographical variability with different decomposition profiles. Some soil samples exhibit preferential decomposition of the labile fraction, while others show the opposite pattern, with faster decomposition of the Exo2 fraction. The evolution of these fractions with increasing depth also indicates different degrees of decomposition of the soil layers from different sites. The reason for this local SOM variability can only be explained by the differing microbial composition of soils (Fukami et al., 2010) and by the different environmental conditions of the samples. Geographical variability of SOM properties as decomposition proceeds is well documented (Pietsch et al., 2019) and thermal and thermodynamics properties of SOM are also sensitive to that (Barros et al., 2020). The results here indicate that although the soil properties may be determined by dominant trees (Urbanová et al., 2015), they can be determined by other factors than the tree species too. All these transformations result in an increase in Q_{SOM} following soil depth indicating the evolution of SOM to a higher degree of reduction (Fig. 3), as reported in previous papers using soils from oak forests (Barros et al., 2020).

Proximate analysis enriches the previous information about SOM by its fractionation in volatile matter, VM, fixed carbon, FC, and ash, A. This fractionation is a regular procedure for the energetic characterization of biomass and the characterization of biochars obtained by pyrolysis (Hasan et al., 2018). Recent literature provides information about these properties of the matter for different vegetation and organic materials (Bilen, 2019; Reyes et al., 2021; Stasiak et al., 2017) and also for soil fertilizers such as biochars (Klasson, 2017), but the applicability to soil is not well documented yet. The soil samples studied in this paper show higher volatile matter than fixed carbon percentages, as reported for other organic vegetal materials (Chouchene et al., 2010). This prevalence is preserved along with soil evolution with depth. There is, however, a clear trend of the volatile matter to increase and the fixed carbon to decrease as SOM mineralizes (increasing soil depth). These values are in the expected range reported for many organic substrates (García et al., 2012), settling values for the volatile matter from 65% to 85% (Yang et al., 2005). The fixed carbon is usually highly variable in the literature, which is explained by the fact that it is an indirect measurement (García et al., 2012). In this paper, the fixed carbon, is directly determined from the soil mass remaining after the pyrolysis, yielding values not significantly different from those indirectly obtained by equation (6). Therefore, the observed variability cannot be due to the method. Values of the volatile matter and the fixed carbon reported for oak tree leaves are 72 and 24.19% respectively (García et al., 2012), which are close to the values obtained for the mineral soil samples in this work. Most organic samples (LF and H) have values for the fixed carbon ranging from 62.67 to 20.19%, with a trend to decrease as mineralization proceeds. Ash clearly increases with soil mineralization, and in most of the soil samples, the ash percentage is higher than the range reported for different forest biomass (García et al., 2012; Telmo et al., 2010). High ash content usually disables organic resources as sources of energy. It is associated by the literature to high contents of labile organic and inorganic compounds. The clear increase here can be a consequence of the higher degree of SOM mineralization as soil depth increases, and to higher interaction of SOM with mineral soil elements. Therefore, the ash content in soil could be attributed to the SOM reactivity to mineral soil components as reported for biochars (Rimena et al., 2017).

The temperatures of the peaks from the pyrolysis are variable among samples but are in the range reported for monosaccharides, cellulose and lignin (Guo et al., 2016), suggesting that these materials are pyrolyzed in the samples. Literature reports cellulose and hemicellulose as the main source of volatile matter (Klasson, 2017). The variability observed for the volatile matter may be probably due to the lower or higher prevalence of each component depending on the degree of decomposition of SOM. The fact that the volatile material increases with soil depth and therefore, with the degree of SOM transformation, can be explained by the increment in aromatic hydrocarbon as products of SOM decomposition, as reported for oak organic matter (Chavez-Vergara et al., 2014).

DSC quantifies the energy of SOM combusted and pyrolyzed. Highly organic substrates usually generate low ash percentages. For that reason, the energy can be measured by normalizing the integral of the DSC plot to the sample mass combusted on a wet or dry basis. This value is usually given as the Higher Heating Value (HHV) because under these experimental conditions organic substrates are combusted to CO_2 and water in the gaseous state. Nevertheless, SOM increases the ash formation after combustion as the degree of soil mineralization rises. Therefore, the energy content of SOM must be normalized to the quantity of SOM combusted given by equation (3), which is not the same as the energy normalized to the initial soil mass. For this reason, the energy content of soil is considered as the heat of combustion of SOM (Q_{SOM}) when normalized to the organic matter content. Q_{SOM} values obtained by airflow in the DSC are given in Table 1. Values for LF and H samples are in the range of Q_{SOM} values given for carbohydrates (15.65 kJ/g) (Gary et al., 1995), cellulose (16.61–17.51 kJ/g) (Blokhin et al., 2011), lignocellulosic material (17.5–18.5 kJ/g) (Stasiak et al., 2017), and oak leaves (17.52 kJ/g) (García et al., 2012). These values increase with soil depth ranging from 17.4 to 21.80 kJ/g SOM in the mineral samples, reflecting the different degrees of decomposition among samples from

different sites but being significantly higher than values in LF samples. These Q_{SOM} values show the evolution of SOM to a more reduced state than carbohydrates as soil depth increases, as reported in previous papers (Barros, 2021; Barros et al., 2020). There are different co-existing theories about SOM evolution without a definite clear trend yet. The debate is about the evolution of SOM to a higher or lower degree of reduction or oxidation as the soil ecosystem evolves (Lehmann and Kleber, 2015). This paper shows SOM at different stages of decomposition from the same forest ecosystem with Q_{SOM} values varying from 17.4 to 21.80 kJ/g SOM in the mineral samples. All of these values are still at a higher degree of reduction than their LF layers (also at different degrees of decomposition). It has been proved that SOM from oak trees at early stages of decomposition gives Q_{SOM} values which are higher than the oak leaves, due to the decomposition of lignin to highly aromatic compounds (Chavez-Vergara et al., 2014). Therefore, the observed variance of Q_{SOM} values in the mineral samples would result from different degrees of transformation of SOM among soil samples. Those with the lowest Q_{SOM} values would evolve following the theories of SOM transformation from large and energy-rich compounds to smaller energy-poor compounds (Lehmann and Kleber, 2015).

The soil mass remaining after pyrolysis combusted under airflow indicated the presence of C and H in the pyrolyzed material, giving mass values not significantly different from FC data obtained by equation (6). The Ash material after the combustion following the pyrolysis was not significantly different from that obtained after combustion with airflow only. Q_{SOM} of the material remaining after the pyrolysis (Table 1) is in every sample higher than Q_{SOM} values obtained from the original SOM. In most of the samples, the obtained values are within the range of the estimates given for different biochars (20–30 kJ/g) (Malucelli et al., 2020) and the amount for pure carbon (35 kJ/g) (Ronsse et al., 2013). But there are samples with values even higher than 35 kJ/g suggesting wood-derived biochar (Crombie and Mašek, 2015).

DSC is a potential method for direct measurement of the energy content in different materials, but when it is not possible to do it by these devices, proximate and elemental analysis can provide an approach to calculate the energy content by multiple regression formulas. There is literature giving different equations connecting the energy of organic substrates with their proximate and elemental composition to facilitate future energy approaches (Hasan et al., 2018; Malucelli et al., 2020). These correlations are also reported among elemental composition and proximate data to determine the stability of biochars which could be an option to be applied to assess SOM stability (Klasson, 2017). In this paper, those correlations were tested too in order to facilitate future soil characterization by these procedures. The soil elemental properties were closely correlated with the SOM, VM, FC, and Ash, making it possible to provide the equations connecting those variables (Table 4) for soil samples from oak ecosystems. The results did not differ very much from the ones reported for different biomass resources (Malucelli et al., 2020; Nhuchhen and Afzal, 2017; Parikh et al., 2007), being C and HHV the most mutable. The reported equations may be useful to be compared to soils from different ecosystems. The fact that soil proximate fractions correlated with HHV makes proximate analysis an alternative approach to estimate Q_{SOM} and the energy stored by the SOM. The last has been proven to allow the complete thermodynamic characterization of SOM (Barros, 2021; Barros et al., 2020).

The VM/FC ratio was determined here to assess the sensitivity of the proximate fractions to SOM evolution with depth. Application to biochar relates this ratio with biochar stability. Material with a VM/FC ratio higher than 0.88 is considered less stable with a lower half-life (Klasson, 2017). All these soil samples with only one exception (sample F5–H) have a higher VM/FC ratio than 0.88, indicating less stable SOM than biochar. This ratio is, however, very variable in the M samples suggesting that SOM decomposition may lead to a more or less stable organic matter. It would be of interest to explore the reliability of these ratios as an alternative to parametrize SOM stability and recalcitrance.

5. Conclusions

Proximate analysis of soils improves, and complements results obtained by traditional thermal analysis under airflow.

VM, FC and Ash present better correlations with soil elemental components and energy data than the traditional soil Exo thermal fractions at combustion conditions in the TG-DSC. Nevertheless, these Exo thermal fractions under airflow allow better monitorization of SOM evolution than VM and FC in terms of the progression of the labile and recalcitrant SOM components.

Proximate analysis of soils can provide equations to obtain the energy content of soils and may be explored as possible tools to inform about SOM stability. The obtained connection between the HHV and the proximate fractions make this method an additional tool for quantifying energy in soil and therefore, towards the SOM thermodynamic characterization.

Funding

This work is funded by the Spanish Ministery of Science and Innovation (PID 2022-119204RB-C22).

Declaration of competing interest

The authors declare that they have no known competing financial interests or personal relationships that could have appeared to influence the work reported in this paper.

Data availability

No data was used for the research described in the article.

Acknowledgements

The authors thank Verónica Piñeiro and Montse Gómez of the RIAIDT analytical services at the University of Santiago de Compostela (Spain) for elemental and thermal analysis. Authors also thank Ken Byrne from the department of Biological Sciences, University of Limerick (Ireland), Eva Vanguelova from the Alice Holt Forest Research Station (UK) and Ander Arias González from Neiker-Tecnalia Basque Institute for Agricultural Research and Development (Spain) for the soil samples supply. This work has been developed under the project CONGESTION, funded by the by the Spanish Ministery of Science and Innovation (PID 2022-119204RB-C22).

Appendix A. Supplementary data

Supplementary data to this article can be found online at https://doi.org/10.1016/j.envres.2023.115310.

References

Almendros, G., González-Vila, F.J., 2012. Wildfires, soil carbon balance and resilient organic matter in Mediterranean ecosystems. A review. Span J Soil Sci 2, 8–33.

Barros, N., 2021. Thermodynamics of soil microbial metabolism: applications and functions. Appl. Sci. 11, 4962. https://doi.org/10.3390/app11114962.

Barros, N., Fernandez, I., Byrne, K.A., Jovani-Sancho, A.J., Ros-Mangriñan, E., Hansen, L. D., 2020. Thermodynamics of soil organic matter decomposition in semi-natural oak (Quercus) woodland in southwest Ireland. Oikos 129, 1632–1644. https://doi.org/10.1111/oik.07261.

Barros, N., Salgado, J., Feijóo, S., 2007. Calorimetry and soil. Thermochim. Acta, XIVth ISBC Proceedings Special Issue 458, 11–17. https://doi.org/10.1016/j.tca.2007.01.010.

Bilen, M., 2019. Proximate and ultimate analysis before and after physical &amp$ \mathsemicolon$ chemical demineralization. IOP Conf. Ser. Earth Environ. Sci. 362, 012092 https://doi.org/10.1088/1755-1315/362/1/012092.

Blokhin, A.V., Voitkevich, O.V., Kabo, G.J., Paulechka, Y.U., Shishonok, M.V., Kabo, A. G., Simirsky, V.V., 2011. Thermodynamic properties of plant biomass components. Heat capacity, combustion energy, and gasification equilibria of cellulose. J. Chem. Eng. Data 56, 3523–3531. https://doi.org/10.1021/je200270t.

Chakrawal, A., Herrmann, A.M., Manzoni, S., 2021. Leveraging energy flows to quantify microbial traits in soils. Soil Biol. Biochem. 155, 108169 https://doi.org/10.1016/j.soilbio.2021.108169.

Chavez-Vergara, B., Merino, A., Vázquez-Marrufo, G., García-Oliva, F., 2014. Organic matter dynamics and microbial activity during decomposition of forest floor under two native neotropical oak species in a temperate deciduous forest in Mexico. Geoderma 235–236, 133–145. https://doi.org/10.1016/j.geoderma.2014.07.005.

Chouchene, A., Jeguirim, M., Trouvé, G., Favre-Reguillon, A., Le Buzit, G., 2010. Combined process for the treatment of olive oil mill wastewater: absorption on sawdust and combustion of the impregnated sawdust. Bioresour. Technol. 101, 6962–6971. https://doi.org/10.1016/j.biortech.2010.04.017.

Crombie, K., Mašek, O., 2015. Pyrolysis biochar systems, balance between bioenergy and carbon sequestration. GCB Bioenergy 7, 349–361. https://doi.org/10.1111/gcbb.12137.

De la Rosa, J.M., González-Pérez, J.A., González-Vázquez, R., Knicker, H., López-Capel, E., Manning, D.A.C., González-Vila, F.J., 2008. Use of pyrolysis/GC–MS combined with thermal analysis to monitor C and N changes in soil organic matter from a Mediterranean fire affected forest. CATENA, Fire Effects on Soil Properties 74, 296–303. https://doi.org/10.1016/j.catena.2008.03.004.

Dell'Abate, M.T., Benedetti, A., Brookes, P.C., 2003. Hyphenated techniques of thermal analysis for characterisation of soil humic substances. J. Separ. Sci. 26, 433–440. https://doi.org/10.1002/jssc.200390057.

Dell'Abate, M.T., Benedetti, A., Sequi, P., 2000. Thermal methods of organic matter maturation monitoring during a composting process. J. Therm. Anal. Calorim. 61, 389–396. https://doi.org/10.1023/A:1010157115211.

Fernández, J.M., Plaza, C., Polo, A., Plante, A.F., 2012. Use of thermal analysis techniques (TG–DSC) for the characterization of diverse organic municipal waste streams to predict biological stability prior to land application. Waste Manag. 32, 158–164. https://doi.org/10.1016/j.wasman.2011.08.011.

Fukami, T., Dickie, I.A., Paula Wilkie, J., Paulus, B.C., Park, D., Roberts, A., Buchanan, P. K., Allen, R.B., 2010. Assembly history dictates ecosystem functioning: evidence from wood decomposer communities. Ecol. Lett. 13, 675–684. https://doi.org/10.1111/j.1461-0248.2010.01465.x.

García, R., Pizarro, C., Lavín, A.G., Bueno, J.L., 2012. Characterization of Spanish biomass wastes for energy use. Bioresour. Technol. 103, 249–258. https://doi.org/10.1016/j.biortech.2011.10.004.

Gary, C.C., Frossard, J.S., Chenevard, D., 1995. Heat of combustion, degree of reduction and carbon content : 3 interrelated methods of estimating the construction cost of plant tissues. Agronomie 15, 59.

Guo, F., Wu, F., Mu, Y., Hu, Y., Zhao, X., Meng, W., Giesy, J.P., Lin, Y., 2016. Characterization of organic matter of plants from lakes by thermal analysis in a N2 atmosphere. Sci. Rep. 6, 22877 https://doi.org/10.1038/srep22877.

Hansen, L.D., Popovic, M., Tolley, H.D., Woodfield, B.F., 2018. Laws of evolution parallel the laws of thermodynamics. J. Chem. Thermodyn. 124, 141–148. https://doi.org/10.1016/j.jct.2018.05.005.

Hasan, M., Haseli, Y., Karadogan, E., 2018. Correlations to predict elemental compositions and heating value of torrefied biomass. Energies 11, 2443. https://doi.org/10.3390/en11092443.

Herrmann, A.M., Coucheney, E., Nunan, N., 2014. Isothermal microcalorimetry provides new insight into terrestrial carbon cycling. Environ. Sci. Technol. 48, 4344–4352. https://doi.org/10.1021/es403941h.

Huang, Y., Wang, H., Zhang, X., Zhang, Q., Wang, C., Ma, L., 2022. Accurate prediction of chemical exergy of technical lignins for exergy-based assessment on sustainable utilization processes. Energy 243, 123041. https://doi.org/10.1016/j.energy.2021.123041.

Klasson, K.T., 2017. Biochar characterization and a method for estimating biochar quality from proximate analysis results. Biomass Bioenergy 96, 50–58. https://doi.org/10.1016/j.biombioe.2016.10.011.

LaRowe, D.E., Van Cappellen, P., 2011. Degradation of natural organic matter: a thermodynamic analysis. Geochem. Cosmochim. Acta 75, 2030–2042. https://doi.org/10.1016/j.gca.2011.01.020.

Lehmann, J., Kleber, M., 2015. The contentious nature of soil organic matter. Nature 528, 60–68. https://doi.org/10.1038/nature16069.

Lopez-Capel, E., Sohi, S.P., Gaunt, J.L., Manning, D.A.C., 2005. Use of thermogravimetry–differential scanning calorimetry to characterize modelable soil organic matter fractions. Soil Sci. Soc. Am. J. 69, 930. https://doi.org/10.2136/sssaj2005.0930.

Malucelli, L.C., Silvestre, G.F., Carneiro, J., Vasconcelos, E.C., Guiotoku, M., Maia, C.M. B.F., Carvalho Filho, M.A.S., 2020. Biochar higher heating value estimative using thermogravimetric analysis. J. Therm. Anal. Calorim. 139, 2215–2220. https://doi.org/10.1007/s10973-019-08597-8.

Manning, D.a.C., Lopez-Capel, E., Barker, S., 2005. Seeing soil carbon: use of thermal analysis in the characterization of soil C reservoirs of differing stability. Mineral. Mag. 69, 425–435. https://doi.org/10.1180/0026461056940260.

Merino, A., Ferreiro, A., Salgado, J., Fontúrbel, M.T., Barros, N., Fernández, C., Vega, J. A., 2014. Use of thermal analysis and solid-state 13C CP-MAS NMR spectroscopy to diagnose organic matter quality in relation to burn severity in Atlantic soils. Geoderma 226–227, 376–386. https://doi.org/10.1016/j.geoderma.2014.03.009.

Nhuchhen, D.R., Afzal, M.T., 2017. HHV predicting correlations for torrefied biomass using proximate and ultimate analyses. Bioengineering 4, 7. https://doi.org/10.3390/bioengineering4010007.

Odum, E.P., 1969. The strategy of ecosystem development. Science 164, 262–270. https://doi.org/10.1126/science.164.3877.262.

Parikh, J., Channiwala, S.A., Ghosal, G.K., 2007. A correlation for calculating elemental composition from proximate analysis of biomass materials. Fuel 86, 1710–1719. https://doi.org/10.1016/j.fuel.2006.12.029.

Pietsch, K.A., Eichenberg, D., Nadrowski, K., Bauhus, J., Buscot, F., Purahong, W., Wipfler, B., Wubet, T., Yu, M., Wirth, C., 2019. Wood decomposition is more strongly controlled by temperature than by tree species and decomposer diversity in highly species rich subtropical forests. Oikos 128, 701–715. https://doi.org/10.1111/oik.04879.

Plante, A.F., Fernández, J.M., Leifeld, J., 2009. Application of thermal analysis techniques in soil science. Geoderma 153, 1–10. https://doi.org/10.1016/j.geoderma.2009.08.016.

Reyes, L., Abdelouahed, L., Mohabeer, C., Buvat, J.-C., Taouk, B., 2021. Energetic and exergetic study of the pyrolysis of lignocellulosic biomasses, cellulose, hemicellulose and lignin. Energy Convers. Manag. 244, 114459 https://doi.org/10.1016/j.enconman.2021.114459.

Rimena, R.D., Trugilho, P.F., Silva, C.A., A de Melo, I.C., Melo, L.C.A., Magriotis, Z.M., Sánchez-Monedero, M.A., 2017. Properties of biochar derived from wood and high-nutrients biomasses with the aim of agronomic and environmental benefits. PLoS One 12 (5), e0176884. https://doi.org/10.1371/journal. pone.0176884.

Ronsse, F., van Hecke, S., Dickinson, D., Prins, W., 2013. Production and characterization of slow pyrolysis biochar: influence of feedstock type and pyrolysis conditions. GCB Bioenergy 5, 104–115. https://doi.org/10.1111/gcbb.12018.

Rovira, P., Henriques, R., 2011. Energy content of soil organic matter as studied by bomb calorimetry. In: Goldschmidt Conference Abstracts, p. 1761.

Rumpel, C., Kögel-Knabner, I., 2011. Deep soil organic matter—a key but poorly understood component of terrestrial C cycle. Plant Soil 338, 143–158. https://doi.org/10.1007/s11104-010-0391-5.

Sarangi, P.K., Nanda, S., Mohanty, P. (Eds.), 2018. Recent Advancements in Biofuels and Bioenergy Utilization, first ed. Springer Singapore.

Saurer, M., Siegwolf, R., 2004. Pyrolysis techniques for oxygen isotope analysis of cellulose. In: de Groot, P.A. (Ed.), Handbook of Stable Isotope Analytical Techniques, pp. 497–506. https://doi.org/10.1016/B978-044451114-0/50025-9.

Smith, J.U., Farmer, J., Smith, P., Nayak, D., 2021. The role of soils in provision of energy. Philos. Trans. R. Soc. B. https://doi.org/10.1098/rstb.2020.0180.

Stasiak, M., Molenda, M., Bańda, M., Wiącek, J., Parafiniuk, P., Gondek, E., 2017. Mechanical and combustion properties of sawdust—straw pellets blended in different proportions. Fuel Process. Technol. 156, 366–375. https://doi.org/10.1016/j.fuproc.2016.09.021.

Telmo, C., Lousada, J., Moreira, N., 2010. Proximate analysis, backwards stepwise regression between gross calorific value, ultimate and chemical analysis of wood. Bioresour. Technol. 101, 3808–3815. https://doi.org/10.1016/j.biortech.2010.01.021.

Urbanová, M., Šnajdr, J., Baldrian, P., 2015. Composition of fungal and bacterial communities in forest litter and soil is largely determined by dominant trees. Soil Biol. Biochem. 84, 53–64. https://doi.org/10.1016/j.soilbio.2015.02.011.

Villanueva, M., Proupín, J., Rodríguez-Añón, J.A., Fraga-Grueiro, L., Salgado, J., Barros, N., 2010. Energetic characterization of forest biomass by calorimetry and thermal analysis. J. Therm. Anal. Calorim. 104, 61–67. https://doi.org/10.1007/s10973-010-1177-y.

Yang, Y.B., Changkook, R., Khor, A., Yates, N.E., Sharifi, V.N., Swithenbank, J., 2005. Effect of fuel properties on biomass combustion. Part II. Modelling approach-identification of controlling factors. Fuel 84, 2116–2130.